Dry Metal Forming Open Access Journal

Fast Manuscript Track

Edited by Frank Vollertsen
Available online at elib.suub.uni-bremen.de

www.drymetalforming.de

Dry Met. Forming OAJ FMT 1 (2015) 63–71
Received 5 February 2015; published 10 February 2015

Potentials of Dry Rotary Swaging

M. Herrmann [*1], H. Hasselbruch[2], F. Böhmermann[3], B. Kuhfuss [1], H.W. Zoch[2], A. Mehner[2] and O. Riemer [3]

[1] bi**me** Bremen Institute for Mechanical Engineering, University of Bremen, Badgasteiner Straße 1, 28359 Bremen, Germany
[2] IWT Foundation Institute for Material Science, Badgasteiner Straße 3, 28359 Bremen, Germany
[3] LFM Laboratory for Precision Machining, University of Bremen, Badgasteiner Straße 2, 28359 Bremen, Germany
[*] Corresponding Author / E-mail: herrmann@bime.de, TEL: +49 421 218 64822

Abstract

Rotary swaging is an incremental cold forming process for the manufacture of cylindrical light weight components such as axles and steering spindles and has a wide spread use in the automotive industry. The advantage of rotary swaging is the optimal use of work piece material resources. This is due to material strengthening through strain hardening and the ability to manufacture hollow parts with variable wall thicknesses. However, main drawback is the need for an extensive lubrication to control tool wear, to discharge abrasive particles from the forming zone, and to provide adequate work piece surface quality. The subsequent, inevitable cleaning of the work pieces after manufacture leads to a significant increase of costs per unit. Thus, the development of rotary swaging towards a dry process layout is highly innovative both under economic and ecological aspects. The omission of lubricant provokes fundamentally changed tribological conditions in tool-work piece contact, leading to changes in process forces, increased abrasive and adhesive tool wear and reduced work piece quality. A robust, lubricant free rotary swaging, offering the same product quality as a conventional rotary swaging process with the use of lubricant, therefore implies the control of the modified tribological properties by methodologies substituting the tasks of the lubricant. This work shows an interdisciplinary approach for the development of dry rotary swaging, that comprises the FE modeling and simulation of the rotary swaging process for general process understanding and designing; the micro structuring of the rotary swaging tool surfaces for control of friction and process forces; and the development of tungsten doped a-C:H tool hard coatings for the reduction of abrasive and adhesive wear of the tools.

Keywords: bulk metal forming, dry metal forming, radial forging

NOMENCLATURE

α	= tool angle
α_{eff}	= effective tool angle
β	= step angle
d_0	= initial work piece diameter
d_1	= final work piece diameter
E_{IT}	= elastic indentation modulus
F_A	= axial reaction force
F_R	= radial forming force
F_f	= feed force
f_{st}	= stroke frequency
h	= step height
H	= overall height
h_T	= stroke height
H_{IT}	= hardness
l	= step length
L	= overall length
n	= number of steps
NP	= neutral plane
r_0	= initial work piece radius
r_1	= final work piece radius
RONt	= roundness value
S_a	= roughness
S_o	= wall thickness
v_f	= feed velocity
x	= feed length

*E-mail address of corresponding author: herrmann@bime.de

Δx	= tracking error
μ_{Red}	= friction coefficient in the reduction zone
μ_{Cal}	= friction coefficient in the calibration zone
I	= reduction zone
II	= calibration zone
III	= exit zone

1 Introduction

Rotary swaging is an incremental bulk metal forming process. It allows, amongst others, for the reduction of the diameter of rods and hollow shafts. For the process variant infeed swaging the work piece is axially fed into the swaging unit with a feed force F_f. The incremental forming is carried out by the oscillating movement of the tools with the stroke height h_t. The radial forming force F_R in the reduction zone causes an axial reaction force F_A counteracting the feed force. The principle of infeed rotary swaging is shown in Fig. 1.

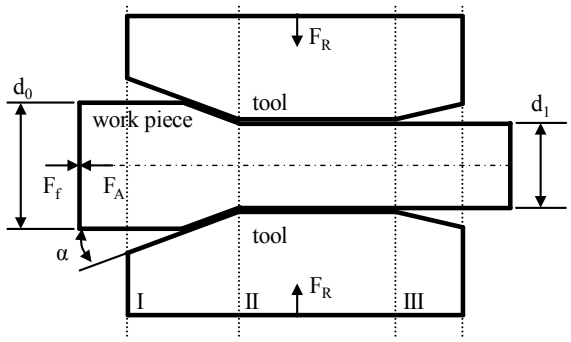

I: reduction zone II: calibration zone III: exit zone

Fig. 1: Cross sectional view of rotary swaging process setup and process forces.

The magnitude of the axial reaction force F_A is determined by the tool geometry, the frictional conditions between the tools and the workpiece as well as the feed velocity v_f. For a tribological adaption of the rotary swaging process towards a reduction of the reaction force, commercially available rotary swaging tools exhibit a layer of tungsten carbide with a rough surface finish in the reduction zone increasing the effective friction between the tools and the work piece. While rotary swaging the tungsten carbide layers tend to clog with wear particles, causing a loss of tribological effectiveness. The clogging can be avoided by extensive lubrication.

Rotary swaging is associated with considerably high process forces and contact pressures per unit area which causes high frictional shear stress in the workpiece material [1]. Furthermore, the work piece surfaces area is increased while forming. And these newly generated surfaces are free of protective oxide layers [2]. Both effects can lead to extensive abrasive and adhesive tool wear, reduce the work piece surface quality or even provoke a damage of the work piece material. The use of lubricant helps providing a robust rotary swaging process, can effectively reduce wear, and ensures the achievement of desired work piece quality through a hydrodynamic separation of tools and work piece. When developing rotary swaging towards a dry process offering the same robustness and work piece quality as a conventional process, methodologies are required that can substitute the versatile functions of the lubricant in rotary swaging.

This work presents an interdisciplinary approach and first research results that can contribute to the successful development of dry rotary swaging. FE modeling and simulation is used for general process understanding and process design. Here, the simulative pre-calculation of process forces and energy demand allows for the understanding of the impact of changed tribological conditions. Structured tool surfaces can be applied to manipulate the friction between the tools and the work piece. The tribological effectiveness of such structures is assigned to their geometrical dimensions and will be investigated on a newly developed test rig mimicking the geometry and impact loads of the real rotary swaging process. Furthermore, tungsten doped a-C:H hard coatings will be applied to the rotary swaging tool surfaces. Due to extreme hardness and the forming of tribolayers under high contact pressures per unit area, these coatings can successfully reduce both abrasive and adhesive wear on rotary swaging tools. An overview on the interdisciplinary approach is given in Fig. 2.

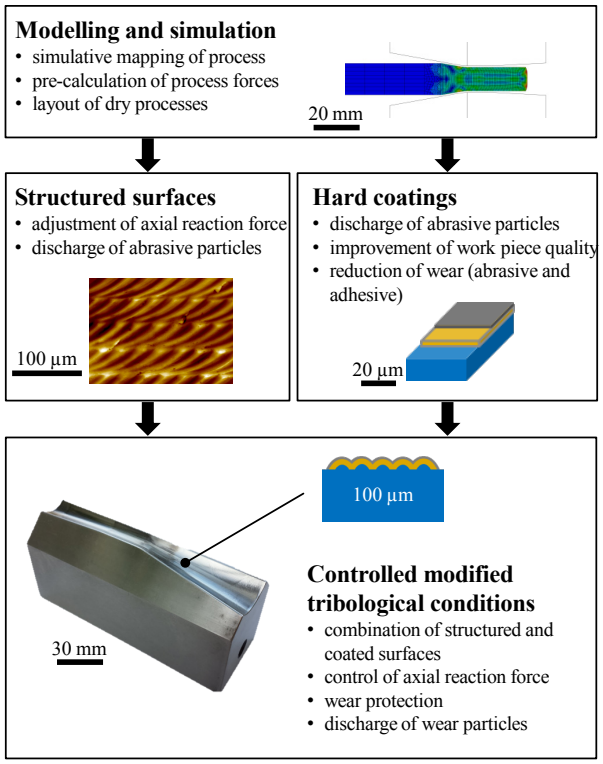

Fig. 2: Interdisciplinary approach for providing a lubricant free rotary swaging process.

2 Experiments

First investigations have been performed with conventional tools which have a layer of tungsten carbide with rough surface finish in the reduction zone. The experiments are executed with a swaging unit *Felss HE-32*. The feeding unit is implemented by a linear direct drive. The workpiece is fed into the swaging unit over a feed length of x = 130 mm. Four different feed velocities are used each with and without lubricant, i.e. wet and dry process conditions. For the dry forming the tools are cleaned each time before the process is started. The hollow shafts of the steel 1.0308 are formed from an average initial diameter of d_0 = 20.028 mm to a final diameter of d_1 = 15 mm. The experimental settings are summarized in Table 1.

Tab. 1: Process settings for the experiments, wet and dry conditions.

parameter	value
tool material	ASP® 2023
workpiece material	Steel (1.0308), cold drawn
length of calibration zone	20 mm
tool angle α	10 °
tool stroke h_T	1 mm
initial diameter d_0	20 mm
final diameter d_1	15 mm
feed velocity v_f	500, 1000, 1500, 2000 mm/min
stroke frequency f_{st}	37.5 Hz
wall thickness s_0	2 mm
average initial diameter	20.028 mm
average initial length	299.85 mm
feed length x	130 mm

The actual and the set value of the feed length are measured continuously during the whole forming process. Thus, the tracking error Δx is calculated by the difference between actual and set value of the feed length. This difference is due to the axial reaction force F_A of the forming process. After the forming process the circularity of the work piece (roundness value RONt) is measured.

For both experiments, wet and dry, the tracking error increases with the feed velocity (see Fig. 3). The tracking error is higher for the wet experiments and additionally the variance for dry rotary swaging is lower. After forming of one hollow shaft without lubricant a large amount of particle abrasion adheres at the surface of the tools. In the reduction zone the particle abrasion cover the layer of tungsten carbide with rough surface finish and can easily be cleaned. For the wet experiment much smaller amount of particle abrasion is observed. The same is noticed for the workpiece where more particles are deposited on the surface after dry forming. Fig. 4 shows the roundness value RONt which is a value for the deviation from the ideal circular shape. The value indicates the distance between the maximal positive and the maximal negative deviation of the perfect circular form (LSC). The roundness deviation increases with higher feed velocities irrespective of the lubricant condition, though the dry formed work pieces exhibit a higher roundness deviation as well as a higher variance. Moreover, the roughness is higher for the workpieces which are formed by dry rotary swaging. It can be summarized, that dry rotary swaging leads to a decrease of the geometric accuracy of manufactured parts.

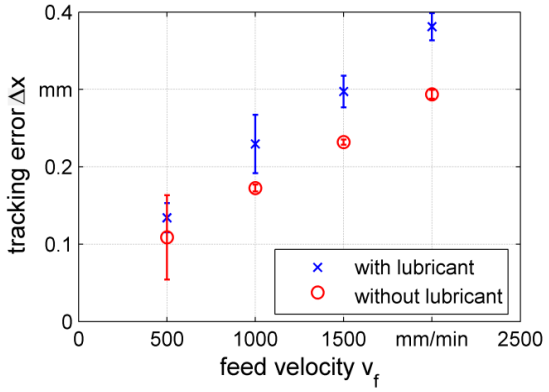

Fig. 3: Tracking error for different feed velocities with/without lubricant.

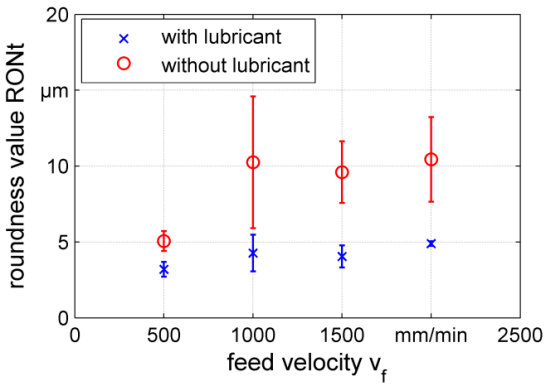

Fig. 4: Roundness value for different feed velocities with/without lubricant.

Thus, the strong influence of the lubricant conditions on rotary swaging has been demonstrated. For dry forming the friction coefficient between tool and work piece is influenced and the value is increased due to the missing lubricating effect. This leads to a lower tracking error for the dry forming process. Furthermore, the high amount of particle abrasion can be explained with the higher friction coefficient during dry forming. Due to the absence of the flushing of the lubricant the particles adhere to work piece and tool. Moreover, the particles lead to a loss in geometric accuracy, i.e. greater roundness deviation. The rising of the roundness deviation with higher feed velocity is due to the higher incremental degree of deformation as well as the shorter

time while the hollow shaft is formed in the calibration zone. Nevertheless, a first process window for dry rotary swaging has been investigated. Dry forming benefits the process parameters tracking error, but due to the particle abrasion and the disadvantageous surface quality of manufactured parts dry rotary swaging needs a modification of the tools. The process window examined serves as a base for comparison to validate tools, which are specially prepared for dry forming.

3 Approaches for a dry process design

The following chapters will give an overview of the modeling and simulation of the rotary swaging process and both tool related approaches, the structuring of tool surfaces, and the use of hard coated tools. Furthermore, first results will be shown towards the development of a lubricant free process design.

3.1 Process modeling and simulation

A further understanding of the rotary swaging process is necessary to define suitable tools and process windows to provide a robust dry forming process. Hence, investigations on the process forces and the energy requirement have been carried out. A comprehensive understanding of the rotary swaging process so far is not given [1], due to the complexity of the process design and a limited accessibility for in-process measurement equipment. A finite element modeling (FEM) of the rotary swaging is of great potential to overcome this limitations and helping to predetermine process forces, strain and stress distribution and material flow in the work piece [3, 4]. Studies acknowledge the existence of the neutral plane (NP), where no axial flow of the material can be detected. The form and position of the NP change during every single stroke [4]. The material before or behind the NP flows in the backward or forward direction, respectively. The distance between the NP and the calibration zone represents the productivity, as e.g. for a large distance a lot of material is formed into the feed direction. Therefore, FE modeling with regard to the NP concept is seen to be one key aspect in the development of the rotary swaging process towards a lubricant free process design. A first effect of simple structures is investigated. Therefore, main attention is paid to the qualitative comparison between the simulation results themselves and advantageous structures for the reduction zone will be identified.

Two-dimensional axisymmetric simulations are commonly used to simulate radial forging processes [3, 4, 5], due to the shorter computational time compared to three-dimensional simulations. First investigation with the simulation model which is used for the following study have been done by Moumi et al. [4]. The 2D-axisymmetric model consisted of two parts, the tool and the work piece and is implemented with Abaqus 6.13-1 (see Fig. 5). The tool is implemented as rigid body and is split in two parts, the reduction zone (I) and the calibration zone (II) including the exit zone (III). As a result different friction coefficients between the work piece and the tool can be set for the different zones. The workpiece is modeled as an elastic-plastic isotropic material and the material behavior is taken from literature [6]. The penalty formulation and the Coulomb friction coefficient is used due to the simplicity and the good results in cold metal forming simulations [7]. Due to the fast dynamic process with incremental forming, the numerical method is based on Abaqus/Explicit. Other parameters are summarized in Table 2.

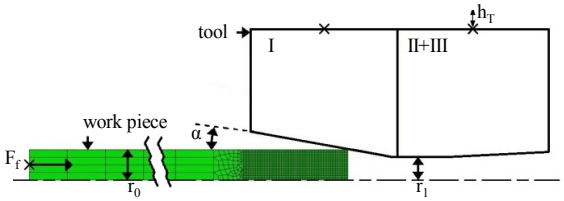

Fig. 5: 2D-axisymmetric model.

Tab. 2: Process parameters for the FE-simulation.

parameter	value
tool angle α	10 °
tool stoke h_T	1 mm
stroke frequency f_{st}	37.5 Hz
initial radius r_0	10 mm
final radius r_1	7.5 mm
number of elements	1350
element type	CAX4R
feed velocity v_f	30 m/s
length of calibration zone	20 mm
material	AISI304

The geometries selected are to gain fundamental insights in basic effects first. The regular structure of steps is in principal defined by n, α_{eff}, β and r. The step length and height h can be derived from the overall length L and height H which are derived from α_{eff} (see Fig. 6). The number of steps n is varied between n = 10 to n = 40 by an increment of two. Thereby the height h and length l are deviated from the fixed overall height H and overall length L due to the fixed effective tool angle which is set to α_{eff} = 10 °. At least the step angle β is varied. For one case the step angle is set to β = 90 °, i.e. this section of the step is perpendicular to the feed direction. For the second case the step height is sloped and the step angle is set to β = 45 °. The edge radius is set to a quarter of the step height h depending on the number of steps through all the simulations. Two different friction coefficients μ - they are taken from literature [8] - are chosen in the reduction zone, where

$\mu_{Red} = 0.5$ represents dry and $\mu_{Red} = 0.1$ represents wet contact, The friction coefficient in the calibration zone is fixed to $\mu_{Cal} = 0.1$.

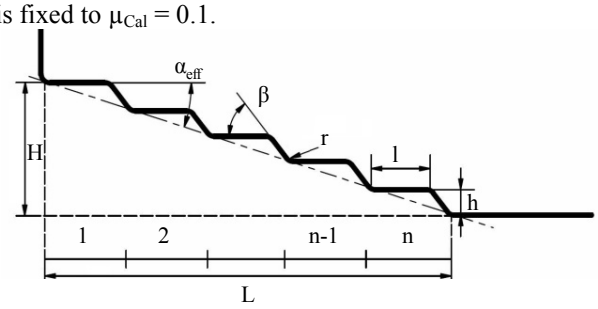

Fig. 6: Example for the geometry of a micro structured tool with number of steps $n = 5$.

An effect on both process forces (F_A, F_R) depending on the number of steps, friction coefficients as well as step angle is evident as shown in Fig. 7 for the axial force and in Fig. 8 for the radial force. The results of the comparative simulation without steps are listed in Table 3. With decreasing number of steps the axial force increases especially for a low friction coefficient due to the sloped step of the structure which generate the main part of the axial force. For a higher number of steps the axial force decreases due to the blocking by the step length l parallel to the feed direction. The radial force is reduced for decreasing number of steps. Higher steps allow more material to flow in the larger space between the surface of the tool and the virtual line of α_{eff} (see comparisons of Fig. 9 b) and Fig 9 c)). Due to this improved material flow the forming is also enhenced and the radial force decreases.

The axial force is influenced more stronglyby the number of steps with a step angle of $\beta = 45$ ° then with a step angle of $\beta = 90$ ° due to the sloped in the structure. The radial force is not significantly influenced by the step angle. For $\beta = 90$ ° the radial forces are slightly smaller due to the larger space generated by the step geometry and the resulting improved material flow (see comparisons of Fig. 9b) and Fig. 9 d)). The distance between the NP and the calibration zone is small for $\beta = 45$ ° and amounts to 25 % (see Fig. 9a)), 35 % (see Fig. 9b)) and 45 % (see Fig. 9c)). This also explains the higher axial force for step angle $\beta = 45$ °.

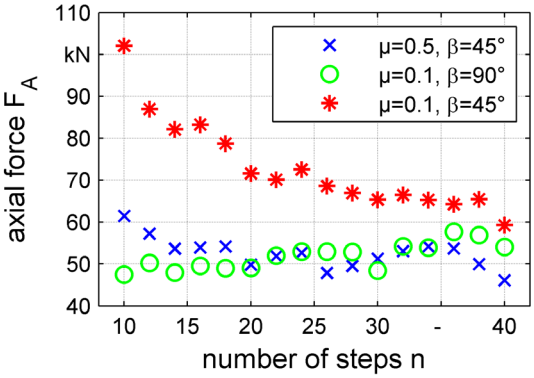

Fig. 7: Axial force on the number of steps.

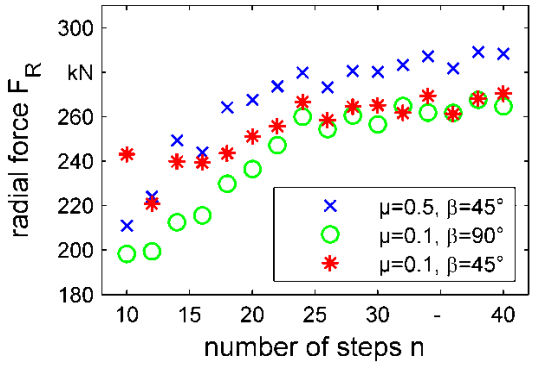

Fig. 8: Radial force on the number of steps.

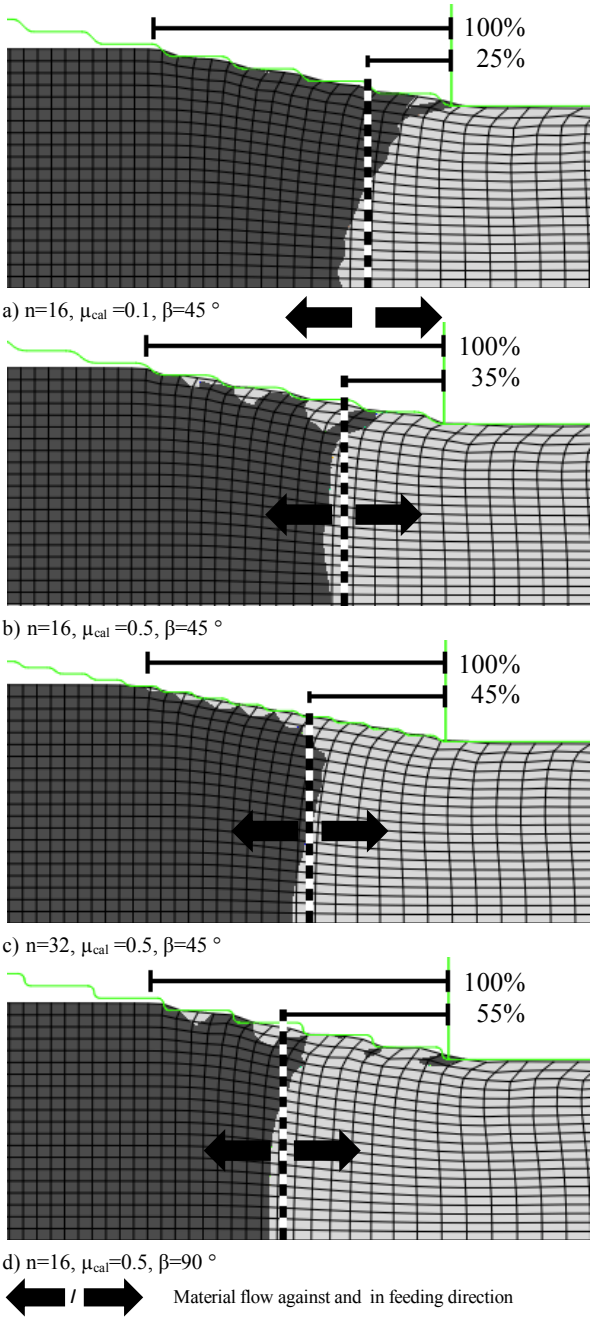

Fig. 9: Influence of the step geometry and friction conditions on the position of the NP.

The simulation results reveal, that structured tools lead to a modification of the process forces as well as the material flow. The radial force decreases with the number of steps whereas the axial force rises especially with a low friction coefficient. On the one hand a step height h radial to the feed direction improves the material flow and the radial force is decreased. On the other hand a step length l parallel to the feed direction reduces the axial force, whereas many sloped increase the axial force especially at low friction. Also the radial force is lower for a large step angle $\beta = 90°$. These findings can be applied advantageously for the design and manufacture of rotary swaging tools.

3.2 Structured tool surfaces

The frictional behavior between forming tools and work pieces can be influenced by structured tool surfaces. The effectiveness of these micro structures can be correlated with their geometrical dimension. Structures of a millimeter and above (macroscopic structures) lead to a change in the direction of forming forces applied on the work piece, as shown by the simulation. A theoretical approach for the application of macroscopic structures to rotary swaging tools with the aim to reduce the axial reaction forces has already been shown [9]. Mesoscopic structures with a feature size of about 50 microns up to a millimeter are used to influence the material flow through elastic deformation of the work piece material in the area of sheet metal forming [10]. Microscopic structures with dimensions of several micrometers usually serve as lubrication reservoirs in forming processes to improve the hydrodynamic separation of tools and the work piece with the aim to reduce friction and wear and to improve the work piece quality [11]. The application of structured tool surfaces to allow for a successful dry metal forming is a complete new approach. Here, extensive fundamental research is required to determine the tribological effectiveness of structured tool surfaces e.g. in dependence on their areal roughness parameters according to ISO 25178 standard. First successful attempts were shown for micro metal forming. Micro structured tool surfaces generated by micro milling exhibited a reduced coefficient of friction compared to polished references in strip drawing tests under dry conditions [12]. The real rotary swaging process is strongly limited regarding the accessibility to measurement of the tribological properties of rotary swaging tools. This is due to the limited accessibility to process forces measurement equipment and the requirement for the manufacture of a new set of tools for each set of experiments. To overcome this limitations a test rig was developed, that mimics typical contact geometries of the tools and the work piece as well as impact loads leading to high contact pressures per unit area. The setup of the test rig is shown in Fig. 10.

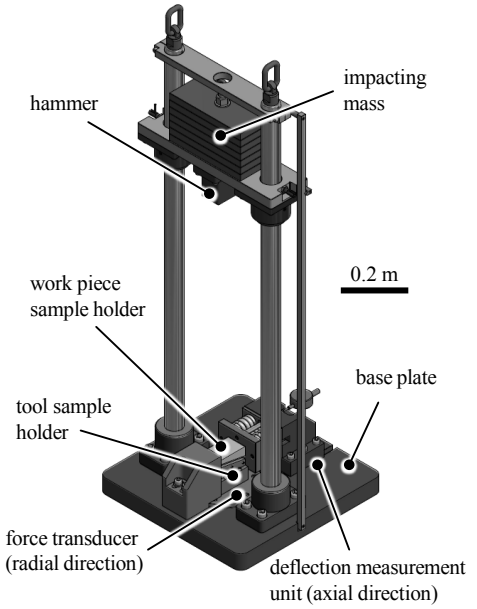

Fig. 10: Setup of the test rig for the tribological investigation of micro structured surfaces.

The principle of the test rig is based on a variable mass to impact on the work piece sample holder containing a sample made from the work piece material. The structured tool sample made from hardened cold working steel is embedded in the tool sample holder and counteracting the work piece sample. The samples are interacting under a tool angle of $\alpha = 10°$ and the effective area of tribological contact is 100 mm^2. The necessary contact pressures per unit area applied through the falling impacting mass to the samples in the experiments have been derived from the simulation results presented in the section above. The test rig allows for the application of contact pressures per unit area in a range from 1300 and 2400 N/mm^2. A detailed overview of the work piece and the tool sample holder as well as the samples is shown in Figure 11.

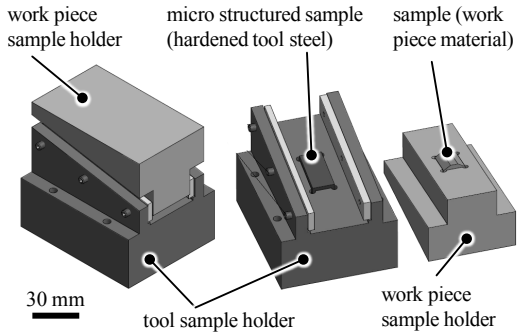

Fig. 11: Assembly of sample holders and samples for the test rig.

The impact of the falling mass (vertical, i.e. the force F_R in radial direction in rotary swaging) causes a horizontal reaction force (axial, i.e. the force F_A in axial direction in rotary swaging). The magnitude of the horizontal reaction force is dependent on the friction between both samples and will be measured by a piezo-electric force transducer or the deflection measurement of the work piece sample holder. The presented test rig will be used for the tribological investigation of structured and hard coated surfaces under the special conditions similar to the real rotary swaging process and, furthermore, will serve for the validation of the simulation results.

3.3 Hard coated rotary swaging tools

Hard coatings, such as CrN, TiN, TiAlN, TiCN or low friction DLC coatings (diamond like carbon) effectively reduce the tool wear in cold forming processes. For lubricant free process conditions the surface roughness and the friction between workpiece and tool surface play a dominant role. In general, coatings with low friction coefficients such as DLC coatings show the best performance as well as promising wear characteristics [13]. This is due to the formation of thin graphitization layers depending on sliding velocities and pressure per unit area, the so-called tribolayer [14]. Another important aspect is the tendency to adhesion depending on chemical adhesion reactions between the DLC coatings and the work piece material and also micro toothing effects due to the topography (roughness) of the coatings in the contact area. Compared to nitride hard coatings, DLC coatings show a lower tendency to cold welding of aluminum and steel [15]. This low adhesion tendency is explained by the saturation of carbon bonds by hydrogen or OH groups on the surface [16]. In addition to the tribological properties also the mechanical properties are of great importance. During rotary swaging dynamic loads with high pressure per unit area and shear stress are applied to the tool's surfaces. Therefore, hard coatings with sufficient fracture toughness are required. High hardness reduces the abrasive wear and the high fracture toughness reduces wear due to fatigue. Diamond like amorphous carbon coatings, as a-C:H stand out especially due to high hardness, low adhesion and low friction in contact with aluminum and steel [17, 18]. But a-C:H-coatings typically show low bearing strength and low overload protection [16]. Therefore, local overloads result in fracture and delamination of a-C:H films [19]. To overcome this so-called "eggshell effect" hard adhesion Cr/CrN-interlayers are used as shown in Fig. 12. A further step to improve the fracture toughness and the resistance against wear due to fatigue is the introduction of an additional a-C:H interlayer doped with tungsten (a-C:H:W) as shown in Fig. 12c. Furthermore, a graded tungsten carbide interlayer acts as a mediator between adhesion layer and the top low friction a-C:H-layer. Doping with tungsten should help to further improve the adhesion and to increase the toughness [20, 21]. A conventional Cr/CrN/a-C:H-layer system is modified stepwise to a tungsten doped multilayer system with an a-C:H functional layer as shown in Fig. 12.

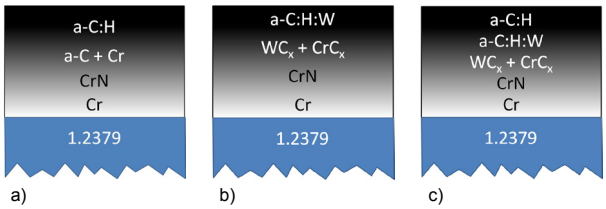

Fig. 12: Different multilayer systems:
a) reference layer Cr/CrN/C+Crx/a-C:H,
b) Cr/CrN/WCx+CrCx/a-C:H:W
c) Cr/CrN/WCx+CrCx/a-C:H:W/a-C:H.

Hardened 1.2379 cold working steel disks with 32 mm diameter and 4 mm thickness were used for the coating experiments. The hardness was 62 ± 2 HRC, what complies with common rotary swaging tool's properties. The specimens were ground, lapped and polished to an average roughness Sa of about 4 nm after the heat treatment. Before deposition, the discs were cleaned in an Amsonic ECS 40 cleaning machine with a precision cleaning medium Zestron® VD. The purification steps include ultrasonic, spray and steam cleaning followed by drying in a vacuum. The deposition was carried out using a CemeCon CC800/9 SinOX magnetron sputtering device with a total of four cathodes. For the reference layer system as shown in Fig. 12a, one cathode was implemented with a chromium target operated in direct current (DC) mode and two cathodes were implemented with graphite targets operated in a bipolar pulsed-DC power mode. For deposition of the layer systems according to Fig. 12b) and Fig. 12c) the fourth cathode was implemented with a tungsten-carbide target operated in DC mode. In total, three different processes were carried out: A Cr/CrN/CrC_x/a-C:H reference layer system without tungsten, a Cr/CrN/WCx+CrCx/a-C:H:W and a Cr/CrN/WCx+CrCx/a-C:H:W/a-C:H layer system with a low friction a-C:H-top layer. All cathodes were operated in power mode with a power of 2 kW, expect for the WC-target, which was operated at 1 kW. The entire process consists of an evacuation and heating phase, a plasma etching phase and several deposition phases depending on the layer systems. The heating started at a base pressure between 1 mPa and 5 mPa and heated with an average power of 15 kW for 1000 s. The plasma etching was carried out under argon respectively krypton atmosphere for 500 s with a pulsed bias voltage

of 650 V. The deposition was carried out at a constant flow of 300 sccm of argon and 75 sccm of krypton. For the deposition of the CrN interlayer a constant nitrogen flow rate of 15 sccm was used. According to VDI 3198, six Rockwell C indentations were performed on each sample to evaluate the adhesion of these four attempts (see Fig. 13).

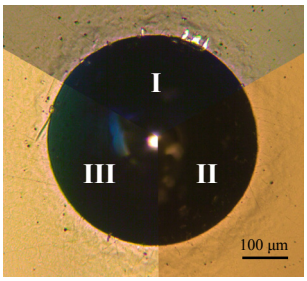

I	a-C:H reference layer
II	a-C:H:W functional layer
III	a-C:H functional layer with a-C:H:W intermediate layer

Fig. 13: Rockwell-C indentation on hard coated samples.

For the determination of the hardness and the elastic indentation modulus a Fischerscope H100C micro hardness measuring system was used. For a statistical coverage 25 measurements for each specimen were performed, whereby the indentation force was 10 mN and the indentation time was set to 10 s. Five ball grinding experiments were carried out on each specimen for coating thickness measurement. The film topography and area roughness were investigated using an atomic force microscope, Explorer Veeco Instruments. For the surface area roughness Sa measurements, one field with dimensions of 100 µm x 100 µm was measured. The results of the experiments are shown in Table 4.

Tab. 4: Experimental results of the different coating variants compared with uncoated 1.2379 steel.

	Uncoated	I	II	III
HF1-6	-	2.0	1.3	1.6
$H_{IT0,01/10/10}$ [GPa]	11.8	21.3	18.0	18.2
$E_{IT0,01/10/10}$ [GPa]	272	190	201	177
thickness [µm]	-	1.77	2.46	1.75
roughness Sa [nm]	3.7	5.3	5.1	5.3

The experimental results confirm that tungsten improves the adhesion and also causes an increase in indentation modulus. The variants II and III are subject of further research. For both variants, the influence of target power (WC), bias voltage and acetylene gas flow will be examined followed by a characterization of the tribological and mechanical behavior of the resulting coating variant. Pin-on-disc tests with steel (1.0038) and aluminum (3.3206) as counter bodies will be conducted in order to characterize the friction and wear behavior of these coatings as a function of processing parameters. Additionally, the impact wear behavior will be determined by impact tests. Rockwell C indentations and scratch tests as well as micro hardness measurements are performed to determine the adhesion, hardness and modulus. Variants showing most promising performance will be subject of further investigations and, finally, the application to rotary swaging tools.

4 Conclusion

Dry forming can be realized by the mastery of the tribological conditions. But due to a lubricant free rotary swaging process design an excessive wear on the tool surfaces and a significant decrease of the work piece quality was observed. Therefore the functions of the lubricant need to be substituted. In this context, novel and interdisciplinary methods for a successful lubricant free rotary swaging are presented. Specifically, these are the structuring of the tool surfaces in the reduction zone and the deposition of tungsten doped low friction a-C:H coatings by reactive magnetron sputtering. On the basis of the swaging experiments it has been demonstrated, that on the one hand dry forming positively affects the tracking error which directly correlates with decreased axial forces. On the other hand, a decrease of the work piece quality was observed by roundness measurements. Additionally, due to the absence of flushing and increased friction, large amounts of wear particles adhered on the work piece and tool surfaces. From the swaging experiments the need of tool modification and the specific tasks of structuring and coating can be derived: First, changing the frictional properties by structured tool surfaces in the reduction zone at different scales and to allow an active discharge of abrasive particles. Second, wear reduction and protection of the structures by the deposition of low friction hard W-DLC coatings.

An evaluation of the process conditions and the process design using modeling and simulation techniques allows for an adaption of the tools` surfaces with regard to the tribological conditions between tool and work piece. A successful implementation of a two-dimensional FE-model of rotary swaging was shown, taking into account various frictional properties and process kinematics which qualitatively confirms the experimental results. Based on the formation and the determination of the neutral plane position the influence of structured tool surfaces were exhibited. Furthermore, input values were obtained for test benches to evaluate the performance of structured tool surfaces and the hard coating. FE-modeling is useful for the adjusting process conditions and to study the impact of structured and/or coated surfaces. For the evaluation of structures with a view to the tribological effectiveness a test rig, mimicking the contact geometries and impact loads of swaging tools and work piece is under development.

Finally, DLC hard coatings show a potential to resolve issues of adhesive tool wear by the work piece as well as the abrasive wear protection for the structured tool surfaces. Particularly, tungsten doped low friction a-C:H coatings provide high hardness for improved abrasion resistance. It is shown that doping with tungsten at the Cr/CrN interface improves the adhesive strength and increases the toughness. The effects of deposition parameters are investigated to further improve the mechanical and tribological properties of both coating variants.

The methods and approaches considered in this work are intended to proceed straight forward to the development and realization of lubricant free rotary swaging processes.

Acknowledgements

The authors would like to thank the German Research Foundation (DFG Deutsche Forschungs-gemeinschaft) for funding this work within the sub-project “Potentials of Dry Rotary Swaging” of the priority program SPP 1676 “Dry metal forming - sustainable production through dry processing in metal forming “.

References

[1] P. Groche, F. Heislitz, “Kraftbedarf beim Kaltrundkneten – Abschlussbericht zum FKM-Vorhaben Nr. 224,“ FKM-Heft, Vol. 224, 2000.

[2] H. Hetzner, “Systematische Entwicklung amorpher Kohlenstoffschichten unter Berücksichtigung der Anforderungen der Blechmassivumformung,“ dissertation, Universität Erlangen, 2014

[3] O. Pantalé, B. Gueye, “Influence of the Constitutive Flow Law in FEM Simulation of the Radial Forging Process,” Journal of Engineering, Vol. 2013, 8 pages, 2013.

[4] E. Moumi, S. Ishkina, B. Kuhfuss, T. Hochrainer, A. Struss, M. Hunkel, „2D-Simulation of material flow during infeed rotary swaging using finite element method,” Proceedia Engineering, Vol. 81, pp. 2342 – 2347, 2014

[5] L. Rong, Z. Nie, T. Zuo, “FEA modeling of effect of axial feeding velocity on strain field of rotary swaging process of pure magnesium.” T. Nonferr. Metal. Soc., 2006; 16: 1015-1020.

[6] E. Doege, H. Meyer-Nolkemper, I. Saeed, Fließkurvenatlas metallischer Werkstoffe, Hanser Verlag, Wien, 1986

[7] X. Tan, “Comparisons of friction models in bulk metal forming.” Tribology I., 2002; 35: 385-393.

[8] H. Czichos, K.-H. Habig, J.-P. Celis, Tribologie-Handbuch: Tribometrie, Tribo-materialien, Tribotechnik, Vieweg + Teubner, Wiesbaden, 2010

[9] N.N., “Forming Tool, in particular Kneading Tool,” International Patent No. WO 2010/105826 A1, date: 18.03.2010.

[10] V. Franzen, J. Witulski, A. Brosius, M. Trompeter, A.E. Tekkaya, “Textured surfaces for deep drawing tools by rolling,” International Journal of Machine Tools & Manufacture, Vol. 50, No. 11, pp. 969-976, 2010.

[11] M. Arentoft, N. Bay, P.T. Tang,J.D. Jensen, “A new lubricant carrier for metal forming,” CIRP Annals - Manufacturing Technology, Vol. 58, No. 1; pp. 243 - 246, 2009.

[12] E. Brinksmeier, O. Riemer, S. Twardy, “Tribological behavior of micro structured surfaces for micro forming tools,” International Journal of Machine Tools & Manufacture, Vol. 50, No. 4, pp. 425 - 430, 2010.

[13] A. Ghiotti, S, Bruschi, “Tribological behaviour of DLC coatings for sheet metal forming tools”, Wear, Vol. 271 , pp. 2454 - 2458, 2011.

[14] Y. Liu, A. Erdemir, E.I. Meletis, “An investigation of the relationship between graphitization and frictional behavior of DLC coating”, Surface and Coating Technology, Vol. 86 - 87, pp. 564 - 568, 1996

[15] M. Murakawa, M. Jin, M. Hayashi, “Study on semidry/dry wire drawing using DLC coated dies”, Surface and Coatings Technology, Vol. 177 - 178 , pp. 631 - 637, 2004.

[16] H. Hetzner, “Systematische Entwicklung amorpher Kohlenstoffschichten unter Berücksichtigung der Anforderungen der Blechmassivumformung,“ dissertation, Universität Erlangen, 2014

[17] P. Carlsson, M. Olsson, “PVD coatings for sheet metal forming processes – a tribological evaluation”, Surface and Coating Technology, Vol. 200, pp. 4654 - 4663, 2006

[18] K. Fujimoto, M. Yang, M. Hotta, H. Koyama, S. Nakano, K. Morikawa, J. Cairney, “Fabrication of dies in micro-scale for micro metal forming”, Journal of Materials Processing Technology, Vol. 177, pp. 639 - 643, 2006.

[19] M. Weber, K. Bewilogua, H. Thomsen, R. Wittdorf, „Influence of different interlayers and bias voltage on the properties of a-C:H and a-C:H:ME coatings prepared by reactive d.c. magnetron sputtering”, Surface and Coatings Technology, Vol. 201, pp. 1576 - 1582, 2006.

[20] X. Chen, Z. Peng, Z. Fu, S. Wu, W. Yue, C. Wang, “Microstructural, mechanical and tribological properties of tungsten-gradually doped diamond-like carbon films with functionally graded interlayers”, Surface & Coatings Technology, Vol. 205, pp. 3631 - 3638, 2011.

[21] A. Czyzniewski, “Optimising deposition parameters of W-DLC coatings for tool materials of high speed steel and cemented carbide”, Vacuum, Vol. 86, pp. 2140 - 2147, 2012.